Interference Models for Heterogenous Sources

Pawel A. Dmochowski*, Peter J. Smith†, Mansoor Shafi‡, Jeffrey G. Andrews§, Rahul Mehta¶
* School of Engineering and Computer Science, Victoria University of Wellington, Wellington, New Zealand
† Department of Electrical and Computer Engineering, University of Canterbury, Christchurch, New Zealand
‡ Telecom New Zealand, Wellington, New Zealand
§ Department of Electrical and Computer Engineering, The University of Texas at Austin, Austin, TX, USA
¶ Radio Spectrum Policy & Planning, Ministry of Economic Development, Wellington, New Zealand
Email: pdmochowski@ieee.org, p.smith@elec.canterbury.ac.nz, mansoor.shafi@telecom.co.nz,
jandrews@ece.utexas.edu, rahul.mehta@med.govt.nz

***Abstract*—Interference modeling is central to the analysis of many interference limited systems. The aggregate interference due to many individual interferers is often very difficult to characterize exactly, especially when lognormal shadowing and path loss is considered. Some results are available for homogeneous sources where the individual components have the same distribution, but many more detailed studies involve heterogeneous sources. Hence, in this paper we build upon previous models for homogeneous sources to develop three general purpose approaches to modeling the aggregate interference from heterogeneous sources which include both shadowing and path-loss. These models are the inverse gamma, inverse generalized gamma and extreme value distributions. These models are motivated by prior work as well as by three distinct interference scenarios relating to cognitive radio systems, digital television and femtocells. The models are fitted to these wide ranging examples and numerical results show good agreement, both for interference and SINR distributions.**

I. Introduction

Interference modeling is central to the design and analysis of wireless systems, since many systems are inherently interference limited. In cellular systems, the dominant performance degradation is usually other-cell-interference. In network MIMO, a complex infrastructure to link base stations is envisaged to manage such interference. In cognitive radio, interference is reduced by a variety of methods to acceptable levels. In spectrum planning, bands of distinct users are established to satisfy out-of-band interference limits. In these examples, simulation can be employed to study the interference, but simulation can be slow, especially at the system level, and does not lead to any insights or further analytical progress. As a result, in this paper we focus on simple statistical models for the total interference power. The statistical models are motivated by extensions of the Levy distribution which appears in certain aggregate interference problems [1]. Also considered are extreme value distribution models which are motivated by observations of real systems and by simulation, where it is observed that a single dominant interferer often accounts for the majority of the total interference.

Our approach considers heterogenous interfering sources as the aim is to build a general approach to the problem and avoid simplifications such as independent identically distributed (iid) sources. The resulting models allow further analysis, such as outage probability and rate calculations. In particular, we use the interference models to derive approximate distributions for the signal-to-interference-plus-noise-ratio (SINR).

Examples are given for three quite different systems. A femtocell system based on [2] is considered as well as a cognitive radio system and a spectrum planning problem where out-of-band cellular interference to a digital television (DTV) system is of interest. These examples are used to motivate both the problem and the solution and numerical results are shown to evaluate the accuracy of the interference models developed.

The contributions of the paper are as follows:

- We motivate and develop three simple models for the aggregate interference from heterogeneous sources where path loss, shadowing and possibly other propagation effects are considered.
- We show that these models provide excellent fits to both interference and SINR distributions in three wide ranging applications of current interest in communications.
- The simplest model, based on an inverse gamma approximation to interference, is shown to provide a remarkably good approximation to interference with only two parameters.

II. System Model

Consider a receiver in the presence of a random number, N, of interferers. The total interference power is

$$I = \sum_{i=1}^{N} I_i, \tag{1}$$

where we are considering the long term interference level, rather than the fast fading version. The N interferers may correspond to different types of source, may have different transmit powers or experience different types of path loss and shadow fading. However, we do assume a broad framework for an individual source. The interference power, I_i, is defined as

$$I_i = A_i L_i d_i^{-\gamma_i}, \tag{2}$$

where A_i is a scaling factor that accounts for transmit power, antenna characteristics, etc. The variable L_i represents lognormal shadowing and is defined by $L_i = 10^{X_i/10}$, where $X_i \sim \mathcal{N}(0, \sigma_i^2)$. Path loss is modeled by the $d_i^{-\gamma_i}$ term, where d_i is the distance from source to receiver and γ_i is the path loss

exponent. All parameters may vary from one user, or group of users, to another.

III. Interference Modeling

In the case of homogenous sources, some results are available. For example, when $A_i = A$ is a constant, $\sigma_i = \sigma$ is fixed and $\gamma_i = \gamma$ is fixed, Hong et al [1] derive the distribution of I in the case where the sources form a Poisson field. This is equivalent to a limiting version of our model where $N \to \infty$. The work in [1] shows that under these assumptions I has a stable distribution. Unfortunately, probability density functions (PDFs) and cumulative distribution functions (CDFs) are only available for stable distributions in a few special cases. One useful example is the scenario where $\gamma = 4$. Here, the stable distribution simplifies to the Levy PDF

$$f_I(y) = \sqrt{\frac{\delta}{2\pi}} \frac{e^{-\delta/2y}}{y^{2/3}}, \quad y > 0, \tag{3}$$

where $\delta = \frac{A}{2}\pi^2\theta^2\Gamma(1/2)e^{\tilde{\sigma}^2/4}$, θ is the density of interfering sources and $\tilde{\sigma} = \log_e(10)\sigma/10$. Hence, the particular scenario of a Poisson field of homogenous interferers with $\gamma = 4$ has the closed form solution given by (3).

A. The Inverse Gamma Model

Since the Levy PDF holds for homogenous sources with $\gamma = 4$, it is reasonable to expect that a broader family of distributions, that includes the Levy, would be a sensible model when γ varies or when homogeneity is relaxed. Hence, we propose the inverse gamma (IG) family as the Levy is a special case of IG with shape parameter equal to $1/2$. To parameterize the IG family, consider the gamma variable X, with shape parameter α and scale parameter β. The IG variable, Y, is defined by $Y = X^{-1}$ and has PDF and CDF given by

$$f_Y(y) = \frac{e^{-1/\beta y}}{\beta^\alpha \Gamma(\alpha) y^{\alpha+1}}, \qquad y > 0, \tag{4}$$

$$F_Y(y) = 1 - \frac{\gamma(\alpha, 1/\beta y)}{\Gamma(\alpha)}, \qquad y > 0, \tag{5}$$

where $\gamma(\cdot,\cdot)$ is the lower, incomplete gamma function.

B. The Inverse Generalized Gamma Model

Continuing with the philosophy of extending the generality of the distribution to increase the range of scenarios modeled, we now extend the IG to the inverse generalized gamma (IGG). If Y has the IG distribution in (4) then $Z = Y^s$ is IGG, for $s > 0$, with PDF and CDF

$$f_Z(z) = \frac{e^{-1/(\beta z)^{1/s}}}{s\beta(\alpha/s)\Gamma(\alpha) z^{\alpha/s+1}}, \qquad z > 0, \tag{6}$$

$$F_Z(z) = 1 - \frac{\gamma(\alpha, 1/\beta z^{1/s})}{\Gamma(\alpha)}, \qquad z > 0. \tag{7}$$

Hence, we have the nested models, Levy, IG and IGG, in order of increasing generality[1].

[1]Since the models are based on extensions of the classic Levy model for a certain class of homogenous interferers, it is likely that they will be useful over a range of scenarios, from purely homogenous to highly heterogenous

C. The Extreme Value Distribution Model

A different approach to interference modeling is given by the extreme value distribution (EVD). This model was motivated by simulations of the DTV receiver, see Sec. IV-B. Here, we observed that the SINR with a single dominant interferer was often very similar to the SINR with total interference. Hence, it is interesting to see if a general model for the maximum interferer, the EVD [3], can also be a useful model for the total interference. Since interference is a positive random variable, we adopt the EVD of type 2 [3], defined by the PDF and CDF,

$$f_W(w) = \frac{k}{\Omega}\left(\frac{\omega}{\Omega}\right)^{-k-1} e^{-\left(\frac{\omega}{\Omega}\right)^{-k}}, \qquad w > 0, \tag{8}$$

$$F_W(w) = e^{-\left(\frac{\omega}{\Omega}\right)^{-k}}, \qquad w > 0, \tag{9}$$

where $k > 0$, $\Omega > 0$ are parameters.

D. Parameter Fitting

Analytical parameter fitting appears to be a complex problem for heterogeneous sources. When the interferers in (1) are not iid, the statistics of I are difficult to evaluate, with the exception of the moments. Unfortunately, the moments of I are not useful for model fitting as shown by the Levy case in [1]. For the homogeneous scenario considered in [1], the Levy distribution is the exact interference distribution. Since the Levy distribution has no moments, fitting via the moments is meaningless. In contrast, if I is Levy then I^{-1} is gamma which can be fitted simply by moment matching. Hence, the nature of the interference distributions is long-tailed, where distributions which fit accurately may not have finite moments. However, numerical fits are straightforward for functions of the interference, eg. I^{-1}. Hence, in this paper we use simulated values of I to perform parameter fitting and leave analytical methods to later work.

For all three proposed distributions, IG, IGG and EVD, we employ the simple method of moments techniques from [4] and [3]. Let m_1, m_2 be the sample mean and variance of the simulated I^{-1} values. For IG, I^{-1} is modeled as a gamma variable and the method of moments gives [4, p.357]

$$\hat{\beta} = m_2/m_1, \qquad \hat{\alpha} = m_1/\hat{\beta}, \tag{10}$$

where $\hat{\alpha}$, $\hat{\beta}$ are the estimates to be used in (4), (5).

For the IGG, we use the log-moments approach [4, p.395]. Let m_1, m_2, m_3 be the sample mean, variance and central third moment of $-\log I$. Then, α, β, s in (6) and (7) are estimated by [4, p.395]

$$\frac{m_3}{m_2^{2/3}} = \frac{\psi''(\hat{\alpha})}{(\psi'(\hat{\alpha}))^{3/2}}, \tag{11}$$

$$\hat{s} = \frac{m_3\psi'(\hat{\alpha})}{m_2\psi''(\hat{\alpha})}, \tag{12}$$

$$\hat{\beta} = \exp\left(m_1 - \hat{s}\psi(\hat{\alpha})\right), \tag{13}$$

where $\psi(\cdot)$ is the psi function and (11) has to be solved numerically.

Finally, for EVD we consider $\log I$ which converts the type 2 EVD to a type 1 which has simple moment fitting defined by [3, p.27]. If m_1 and m_2 are the sample mean and variance of $\log I$ then

$$\hat{\Omega} = \exp\left(m_1 + \psi(1)\sqrt{6m_2}/\pi\right), \qquad \hat{\alpha} = \pi/\sqrt{6m_2}, \quad (14)$$

where $\hat{\Omega}$ and $\hat{k}$ are the parameter estimates for use in (8) and (9).

E. SINR Models

Sections III-A to III-C provide three models for the total interference power. In each case, the corresponding SINR distribution can be computed as follows. Let P be the long term power of the desired signal, I be the total interference in (1) and σ_n^2 be the power of the noise at the receiver. The long term SINR is given by

$$\text{SINR} = \frac{P}{I + \sigma_n^2}. \quad (15)$$

Some straightforward manipulations give the SINR CDF as

$$\mathbb{P}\left(\text{SINR} < x\right) = \int_0^\infty F_P(x(y + \sigma_n^2)) f_I(y)\ dy, \quad (16)$$

where $F_P(\cdot)$ is the CDF of the desired signal power and $f_I(\cdot)$ is the PDF of I. Hence a model for the PDF of I gives the CDF of the SINR as the single integral in (16). Depending on the complexity of (16) it may be possible to compute the CDF in closed form or a single numerical integral may be required.

IV. Example Systems

A. Cognitive Radio

Consider a cognitive radio system with a single primary user (PU) pair and K clusters of secondary (or cognitive) users (SUs), each with N_k active transmitters communicating simultaneously to their respective receivers. The PU-Rx is located at the origin, with the PU-Tx and the centers of the K SU clusters uniformly placed within an annulus surrounding the PU-Rx of inner radius R_0 and outer radius R. The SU transmitters are uniformly located around the cluster center in a circular region of radius r.

The received signal strength for all links is assumed to follow the model in (2). For this example system, we assume a path loss exponent γ common to the PU and all SUs. Thus, the desired signal at the PU-Rx is $P = A_{\text{p}} L_{\text{p}} d^{-\gamma}$, where d is the random distance from the PU-Tx to PU-Rx, and the constant A_{p} is determined by the PU transmit power and antenna gains. Due to their proximity, all N_k SUs within a cluster are assumed to undergo common lognormal shadowing. Thus, the interference to the PU-Rx from each of the SU-Tx is given by

$$I_{k,i} = A_{\text{s}} L_k d_{k,i}^{-\gamma}, \quad (17)$$

where $k \in \{1, 2, \ldots, K\}$ and $i \in \{1, 2, \ldots, N_k\}$ denote the cluster index and SU-Tx index, respectively. In (17), A_{s}, assumed to be equal for all SUs, is determined by the SU transmit power and antenna gains and $d_{k,i}$ is the distance from SU-Tx i in cluster k to the PU-Rx. All links are assumed to be iid so that spatial correlation is ignored.

The scaling parameters A_{p} and A_{s} are chosen to satisfy the SNR criteria for the PU-Tx to PU-Rx and SU-Tx to SU-Rx links, respectively. That is, A_{p} and A_{s} are chosen so that the corresponding SNRs exceed a desired target, SNR_T, with a desired target probability.

Denoting the Gaussian noise at the PU-Rx by $\mathcal{CN}(0, \sigma_{\text{p}}^2)$, using (15), the PU-Rx SINR is given by

$$\text{SINR}_{\text{p}} = \frac{P}{\sum_{k=1}^{K} \sum_{i=1}^{N_k} I_{k,i} + \sigma_{\text{p}}^2}. \quad (18)$$

B. Adjacent Band Operation of DTV and Cellular Systems

In this scenario, we study the interference from a cellular user equipment (UE) to a DTV receiver in an adjacent channel in the 700 MHz band. The close proximity in frequency for these two different systems would result in out-of-band emissions from one system interfering with the desired signal of the other system. Fig. 1 shows the Asia Pacific Telecommunity (APT) digital dividend band and potential out-of-band emissions from cellular system UEs in the adjacent DTV band [5]. A guard band between the frequency bands of the two services is intended to limit the extent of out-of-band interference; agreed values of the guardband are shown in Fig. 1 [5]. The system model is illustrated in Fig. 2. DTV

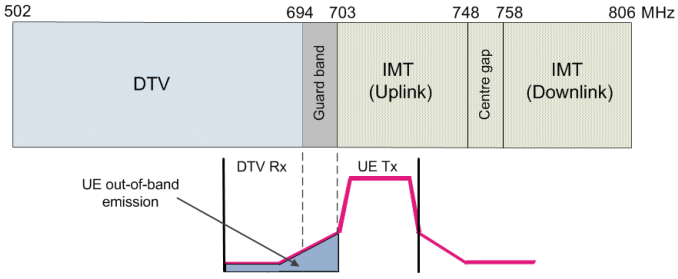

Fig. 1. APT digital dividend band and UE out-of-band emissions.

receivers are uniformly distributed in the coverage area of a DTV transmitter. The DTV coverage area is modeled as an annulus with inner radius R_0 and outer radius R. The UEs are randomly distributed in an annulus around the DTV receiver with inner radius R_1 and outer radius R_2. The active number of UEs around a DTV receiver is a Poisson random variable with a mean density of θ.

The received signal strength for the DTV-Tx to DTV-Rx link is assumed to have the same form as (2), where the constant, A_i, is determined by the DTV transmit power and antenna gains.

The interference to the DTV-Rx from each of the UEs is also consistent with (2) where A_i is a scaling factor that accounts for the UE transmit power and antenna characteristics. Due to the near-far problem in the uplink of cellular systems, power control has been applied to the UEs and is incorporated in the A_i factor. L_i and γ_i could take a number of possible values dependent on the distance between the UE and DTV-Rx.

An out-of-band attenuation factor, g, is applied to the total UE signal power to calculate the interfering signal power for a DTV-Rx. The out-of-band attenuation factor is dependent on the size of the guard band and the channel bandwidths of the UE and DTV-Rx.

Denoting the Gaussian noise at the DTV-Rx by $\mathcal{N}(0, \sigma^2_{\text{DTV}})$, the SINR at the DTV-Rx is given by

$$\text{SINR}_{\text{DTV}} = \frac{P}{g \sum_{i=1}^{N} I_i + \sigma^2_{\text{DTV}}}. \tag{19}$$

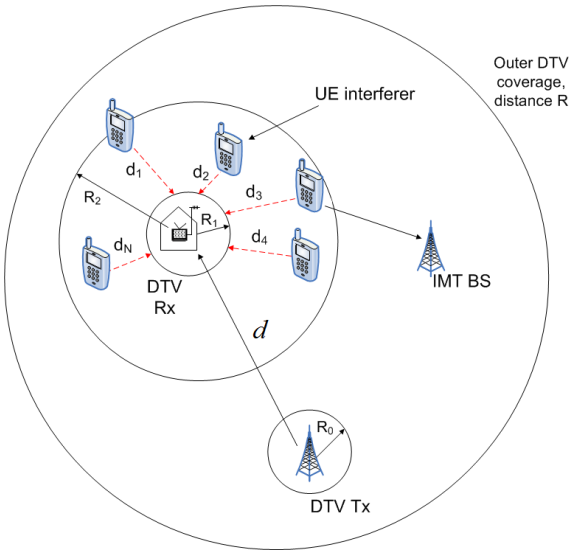

Fig. 2. DTV and Cellular service system diagram.

C. Femtocell

Femtocells – low power, 3rd party miniature base stations – are rapidly being added to cellular networks in an ad-hoc fashion, to enhance their capacity and coverage [6]. By 2014, there will be as many as 50 million femtocells installed worldwide, which will be at least 20 times more than the number of traditional high power base stations [7]. The proposed SINR framework can significantly ease the analysis of even complex models for such two-tier networks.

Although recent progress has been made in finding tractable and near-exact expressions for downlink SINR in such networks [8], [9], these results generally assume Rayleigh fading (and no shadowing), no noise, and other simplifications, whereas the framework proposed here provides easily computable approximations for a broader set of system parameters. Here, for example, we include per-tier lognormal shadowing, a wall loss χ (as appropriate), noise and the possibility of different path loss exponents for the two tiers. We consider the SINR statistics of the macro user, where the macro user is outdoors and the femto user is indoors.

We consider a macrocell user at the origin (without loss of generality) and assume the macrocell BSs follow a 2-D Poisson Point Process (PPP) Φ_{m} with intensity λ_{m}, and the femtocells are drawn from a 2-D PPP Φ_{f} with (usually higher) intensity λ_{f}. We emphasize that although we use the PPP here for ease of exposition, one could just as easily use a hexagonal grid or another preferred spatial model for the base station locations. It is generally agreed that a PPP is a good model for femtocells (which are expected to be nearly iid in space). If the user connects to a macro BS B_0 which is at some location x, the SINR can be modeled as

$$\text{SINR}_{\text{m}} = \frac{P_{\text{m}} L_0 |x|^{-\gamma_{\text{m}}}}{\sum\limits_{i \in \Phi_{\text{m}}/B_0} P_{\text{m}} L_i |Y_{\text{m},i}|^{-\gamma_{\text{m}}} + \sum\limits_{i \in \Phi_{\text{f}}} P_{\text{f}} \chi L_i |Y_{\text{f},i}|^{-\gamma_{\text{f}}} + \sigma^2_{\text{m}}}, \tag{20}$$

where subscripts m and f refer to macro and femto-specific values, L_i is a lognormal shadowing value, and Y denotes the locations of various interfering base stations. In (20), P_{m} and P_{f} denote transmit powers, γ_{f} and γ_{m} denote the path loss exponents and σ^2_{m} is the noise power. The first two terms in the denominator of (20) represent the aggregate interference, which are analyzed in Section V.

The SINR CDF (i.e. the outage probability) of a macrocell user with open access is then

$$F_{\text{m}}(T) \quad = \quad q_{\text{m}} \mathbb{E}_x[\mathbb{P}[\text{SINR}_{\text{m}}(x) \leq T]] \tag{21}$$

where q_{m} is the probability that a randomly located user in the network receives the strongest average signal from a macrocell BS. This *association probability* can be computed, with the simplification that $\gamma_{\text{f}} = \gamma_{\text{m}} = \gamma$, to give [9]

$$q_{\text{m}} \quad = \quad \frac{\lambda_{\text{m}} P_{\text{m}}^{\frac{2}{\gamma}}}{\lambda_{\text{f}} P_{\text{f}}^{\frac{2}{\gamma}} + \lambda_{\text{m}} P_{\text{m}}^{\frac{2}{\gamma}}}. \tag{22}$$

The CDF of the SINR_{m} numerator can be derived using the procedure of Hanif et al [10] with the key difference that the distance CDF, i.e. $F_X(x)$, is now modified because the statistics for macrocells and femtocells affect one another. For example, in open access, densely deployed femtocells decrease the average distance of *both* a femtocell and macrocell connection, since femtocells look increasingly attractive compared to a more distant macrocell BS. Adapting Lemma 2 in [9], one can obtain the CDF for the distance to a macrocell in open access as

$$F_{\text{m}}(x) = 1 - \frac{2\pi\lambda_{\text{m}}}{q_{\text{m}}} \int_x^{\infty} r \exp\left(-\pi \left[\lambda_{\text{m}} r^2 + \lambda_{\text{f}} \hat{P}^{\frac{2}{\gamma_{\text{f}}}} r^{\frac{2}{\hat{\gamma}}}\right]\right) dr, \tag{23}$$

where $\hat{P} = P_{\text{f}}/P_{\text{m}}$ and $\hat{\gamma} = \gamma_{\text{f}}/\gamma_{\text{m}}$. Note that the development in (20)-(23) for a macro user can also be reproduced for a femto user. The SINR CDF can be computed from (16) by employing the relevant interference PDF for IG, IGG or EVD and using the CDF of the desired signal power, which is obtained by using (23) in the procedure of Hanif et al [10].

V. Simulation Results

In order to evaluate the accuracy of the models, we present simulation results for the CDFs of total interference, I, and SINR for the three example systems considered in Sections IV-A, IV-B and IV-C. For interference, we also plot the

empirical CDF of I and compare it to the fitted CDFs of the IG, IGG and EVD distributions given by (5), (7) and (9), respectively. For SINR, we present the CDFs of the resulting SINR from (16), where the interference pdf $f_{\mathrm{I}}(\cdot)$ is obtained from (4), (6) and (8). In the CR and DTV models the CDF, $F_{\mathrm{p}}(\cdot)$, of the desired signal in the form of (2) is computed analytically using (6) in [10]. Note that SINR CDFs for the femtocell application are not included for reasons of space.

Figures 3 and 4 present the CDFs for the CR cluster system described in IV-A. Specifically, we consider a PU coverage radius of $R = 1$ km, with $K = 20$ clusters of $N_k = 5$ SUs each, and SU coverage radius of $r = 20$ m. The PU protection radius is $R_0 = 10$ m. The lognormal shadowing and distance attenuation follow the Hata model [11] where the combined path loss in dB is given by

$$\mathsf{PL} = 124 + 35 \log_{10} d + X, \tag{24}$$

where X is a lognormal variable with $\sigma = 8$ dB and d is in kms. The constants A_{p} and A_{s} are chosen so that the target, $\mathsf{SNR}_T = 10$ dB, is exceeded with a probability of 95%, assuming PU and SU receive antenna gains of 10 dB and 0 dB, respectively. All three models fit the interference data quite well with the EVD the least accurate. The IG and IGG are very similar with the IG a better fit in the lower tail. The accuracy of these models is tested in Fig. 4, where they are used for SINR outage calculations. Here, all three models perform very well. It is surprising that such a simple model as the IG performs so well over the whole range for both interference and SINR.

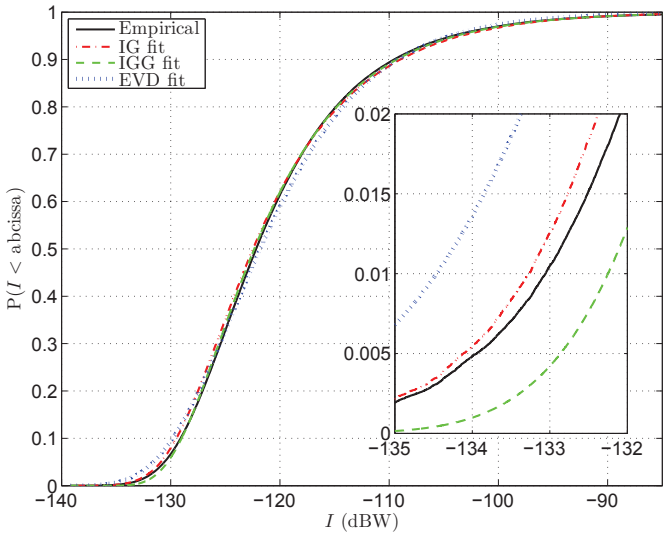

Fig. 3. CDFs of I for the CR model.

Figures 5 and 6 show the corresponding results for the DTV model described in Section IV-B. The parameters used are consistent with those agreed by the Correspondence group of the APT Wireless Group (AWG) [12]. A DVB-T system with a channel bandwidth of 8 MHz and outer coverage radius of $R = 16$ km, inner radius of $R_0 = 1$ km was considered as the DTV system. A UE channel bandwidth of 5 MHz was

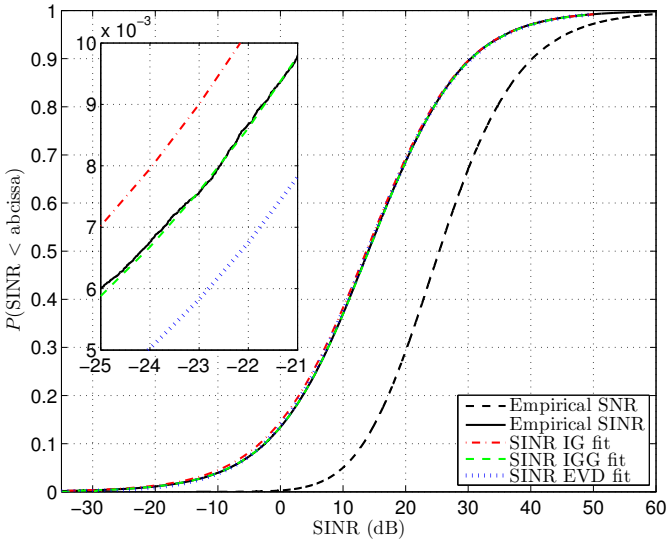

Fig. 4. CDFs of SINR for the CR model.

considered. The Adjacent Channel Leakage Ratio (ACLR) and Adjacent Channel Selectivity (ACS) for the IMT UE and DTV-Rx were obtained from [12]. The outer radius of UE interferers is $R_2 = 1.5$ km and a DTV-Rx protection radius of $R_1 = 10$ m has been used. The lognormal shadowing and path loss for the UE to DTV-Rx link and UE to BS link follow the free space and modified Hata model in [11]. The path loss model used for the DTV-Tx to DTV-Rx link is adapted from the empirical propagation curves in [13].

An out-of-band emission limit of -30 dBm/MHz has been used for the UEs. Fig. 6 illustrates that there is a nominal effect on the DTV-Rx signal from out-of-band emissions of a 5 MHz UE. Table I includes the simulation results on the effect of UE out-of-band interference on DTV coverage. A smaller UE density has been used for larger channel bandwidths since each UE would be using more frequency resources from a fixed spectrum band. The DTV-Rx SNR threshold of 20 dB was agreed by the AWG Correspondence group. Without any interference, the coverage area loss was 1.20%. Column 5 in Table I includes the coverage area loss in addition to these 1.20% of locations that were already in outage. These results show that the effect of UE out-of-band interference on DTV coverage is relatively small. Results for the DTV system are almost identical to those in Figs. 3 and 4. Again, IG and IGG are better models then EVD and IG is impressive in its accuracy for a two parameter model.

TABLE I
INTERFERENCE ANALYSIS RESULTS FOR DTV COVERAGE

UE Bandwidth	UE density (UEs/km^2)	CDF Value @ 20dB SINR	Overall Area Coverage	Coverage Area Loss
5 MHz	13	1.72%	98.28%	0.52%
10 MHz	13/8	1.23%	98.77%	0.03%
15 MHz	13/8	1.30%	98.70%	0.10%

Figure 7 shows the interference results for the open access femtocell model described in Section IV-C. Specifically, we

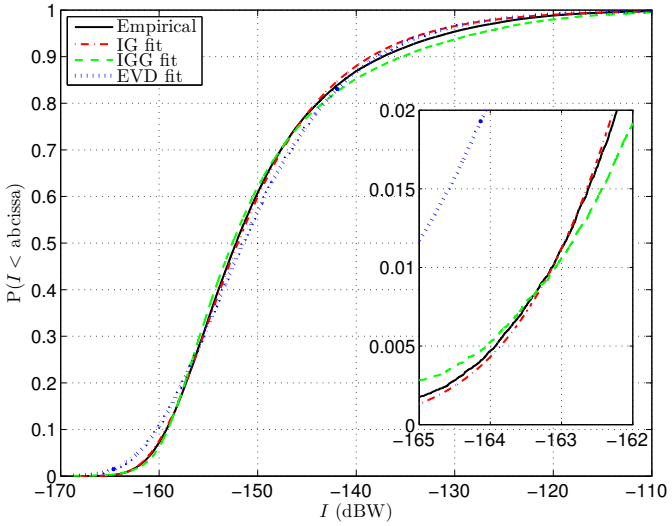

Fig. 5. CDFs of I for the DTV model.

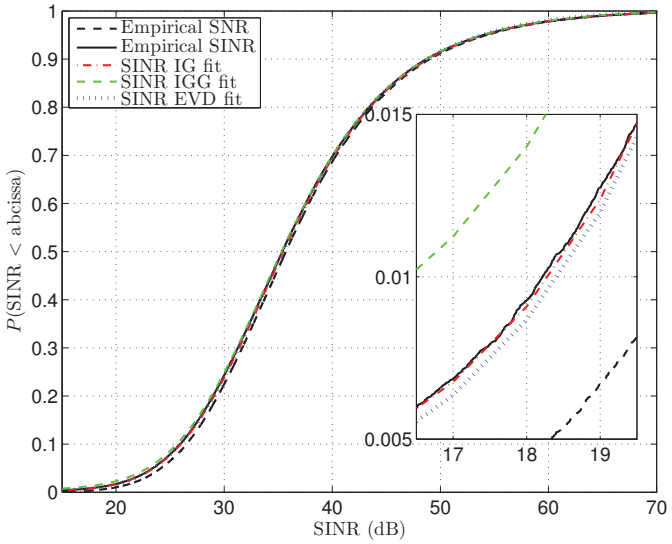

Fig. 6. CDFs of SINR for the DTV model.

consider an open access system with a macro cell radius of $R = 1$ km, wall penetration loss $\chi = 6$ dB, and a normalised femtocell PPP intensity of $\lambda_{\rm f}/\lambda_{\rm m} = 5$. The path loss exponent was set to $\gamma = 3.5$ for both the femto and macro users. Figure 7 again verifies the excellent fit offered by the models, especially IG and IGG.

Although the IGG model has an extra parameter compared to IG, the fits in Figs. 3, 5 and 7 are not, subjectively, better than IG. This is because the IGG also fits the third moment and is therefore more driven by the tails of the distribution. Hence, the IG and IGG fits are different in nature and we do not necessarily see an improvement in the use of IGG.

VI. Conclusions

Analyzing interference and SINR is a complex problem when the interfering sources are heterogeneous. Hence, we have proposed three models, the IG, IGG and EVD distributions, for interference which can also be used in SINR calculations. These models have been motivated and applied to three widely varying communication systems where heterogeneous interference is encountered. In all cases, the EVD model was least effective and the IG/IGG models were very accurate. Due to its simplicity as a two parameter model, the IG model is an extremely attractive approach for interference modeling and has proven to be remarkably accurate.

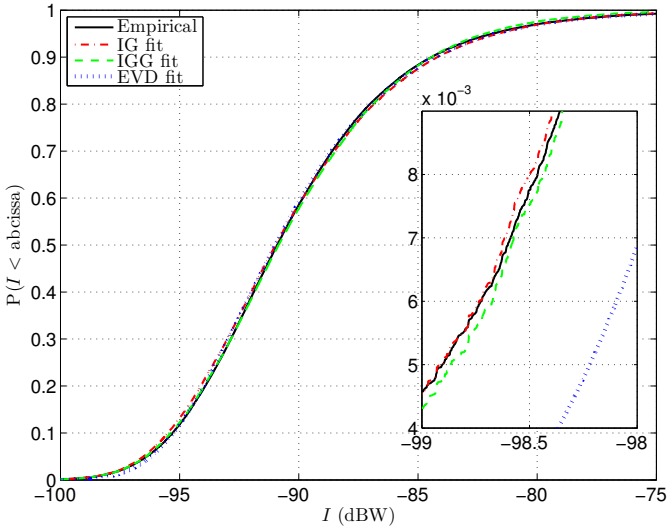

Fig. 7. CDFs of I for the Open Access Femtocell model.

References

[1] X. Hong, C. Wang, and J. Thompson, "Interference modeling of cognitive radio networks," in *Proc. IEEE Vehicular Technology Conference (VTC Spring)*, Singapore, May 2008, pp. 1851–1855.

[2] H. Jo, P. Xia, and J. Andrews, "Downlink femtocell networks: Open or closed?" in *Proc. IEEE International Conference on Communications (ICC)*, Kyoto, June 2011, pp. 1–5.

[3] N. Johnson, S. Kotz, and N. Balakrishnan, *Continuous Univariate Distributions, Vol. 2*. John Wiley and Sons Inc., 1995.

[4] ——, *Continuous Univariate Distributions, Vol. 1*. John Wiley and Sons Inc., 1994.

[5] APT Wireless Group, "Out-of-band emission limits for IMT UE operation in the 700 MHz band," APT Wireless Group, Tech. Rep. AWG-11/INP-76 (Rev.1), 2011.

[6] V. Chandrasekhar, J. G. Andrews, and A. Gatherer, "Femtocell networks: a survey," *IEEE Communications Magazine*, vol. 46, no. 9, pp. 59–67, September 2008.

[7] J. G. Andrews, H. Claussen, M. Dohler, S. Rangan, and M. C. Reed, "Femtocells: Past, present, and future," *To appear, IEEE Journal on Sel. Areas in Comm.*, Mar. 2012.

[8] H. S. Dhillon, R. K. Ganti, F. Baccelli, and J. G. Andrews, "Modeling and analysis of k-tier downlink heterogeneous cellular networks," *To appear, IEEE Journal on Sel. Areas in Comm.*, Mar. 2012.

[9] H.-S. Jo, Y. J. Sang, P. Xia, and J. G. Andrews, "Outage probability for heterogeneous cellular networks with biased cell association," *IEEE Globecom*, Dec. 2011.

[10] M. Hanif, M. Shafi, P. Smith, and P. Dmochowski, "Interference and deployment issues for cognitive radio systems in shadowing environments," in *Proc. IEEE International Conference on Communications*, Dresden, June 2009, pp. 1–5.

[11] ITU-R, "Monte Carlo simulation methodology for the use in sharing and compatibility studies between different radio services or systems," Tech. Rep. ITU-R SM.2028-1, 2001.

[12] APT Wireless Group, "Parameters and propagation models for DTV and IMT in the 700 MHz band," 2011.

[13] ITU-R, "Method for point-to-area predictions for terrestrial services in the frequency range 30 MHz to 3000 MHz," Tech. Rep. ITU-R P.1546-4, 2009.